RESEARCH ARTICLE

Studies towards potential use of ultrasonics in hydrodynamic cavitation control

V. H. Arakeri and S. Chakraborty
Department of Mechanical Engineering, Indian Institute of Science, Bangalore 560 012, India

Hydrodynamic cavitation is well known for its destructive capabilities like material damage and generation of intense noise. For these reasons, except for some special applications, it is to be avoided or controlled. In the present article, we propose the use of ultrasonics towards this goal. The concept of two devices, namely, ultrasonic nuclei manipulator (UNM) and ultrasonic pressure modulator (UPM) has been introduced. Extensive use of solutions to the bubble dynamics equation has been made to arrive at the operating parameters of UNM and UPM. These have been suggested as a frequency of 0.1 MHz and pressure amplitude of 5 bars for UNM and a frequency of near 1 MHz and the same pressure amplitude for UPM. On this basis experiments can be devised to verify the proposed techniques of hydrodynamic cavitation control.

CAVITATION is a term used to describe formation and disappearance of voids or cavities in a body of liquid due to pressure changes. In most cases, one is concerned with a 'cold' fluid in the sense that temperature changes associated with the physical processes of cavity dynamics are sufficiently small to be ignored. If the cavity contains, primarily, the vapour of the liquid, it may be termed vaporous cavitation and if it contains, primarily, a permanent gas then it may be termed gaseous cavitation. The former is a much more violent process and can result in many of the physical effects associated with cavitation like material damage, noise radiation, light emission (termed as sonoluminiscence), etc.[1] Depending on the method by which pressure changes occur in a body of fluid, resulting in the observed cavitation, one may make a further distinction between 'acoustic cavitation' and 'hydrodynamic cavitation'. In acoustic cavitation, the pressure changes are generated with the help of a transducer (typically piezoelectric) and the frequencies involved are generally high being in the ultrasonic range. In hydrodynamic cavitation, the pressure changes are generated due to flow of a fluid past an obstacle or they can exist in cores of turbulent vortices; in either case the equivalent frequencies are low.

In both types of cavitation mentioned, it is now well accepted that cavitation originates from weak spots in the body of the liquid which is subjected to pressure changes. These weak spots are termed 'nuclei' and a good working model for a nucleus is an undissolved spherical gas bubble of radius R_n. For a given nuclei size, R_n, there is a well-defined pressure threshold, P_t for which vaporous cavitation will be possible. In the limit, $R_n \to \infty$, the threshold pressure is the vapour pressure at the bulk temperature of the liquid. For very small size of R_n, like 1 μm, the P_t value is negative, implying that actual tensions are required to initiate vapourous cavitation. Therefore, in acoustic cavitation, where the pressure fields are well defined from the transducer characteristics, the central problem in determining the conditions for the initiation or onset of vaporous cavitation is the knowledge of the nuclei content of the liquid sample. Whereas, in the case of hydrodynamic cavitation, in addition to the knowledge of the nuclei content, determining the characteristics of the pressure field also pose difficulties. Even though considerable efforts have been expended in trying to understand the conditions for the onset of hydrodynamic cavitation in a given situation, relatively less efforts have been devoted to devise means of controlling or eliminating hydrodynamic cavitation. The latter is the focus of present article; however, we first consider certain features of hydrodynamic cavitation which make it undesirable.

Features of hydrodynamic cavitation

A simple device, known as venturi, can be used to generate hydrodynamic cavitation and its geometry is depicted in Figure 1,*a*. The ideal static pressure variation in the device is shown in Figure 1,*b*. The throat pressure, which is the minimum pressure, denoted by p_{min}, can be computed in terms of the geometric and upstream physical parameters using the Bernoulli equation; the result is,

$$p_{min} = p_0 + \frac{1}{2}\rho\left[\frac{Q}{A_0}\right]^2\left[1-\left[\frac{A_0}{A_t}\right]^2\right]. \qquad (1)$$

Here, p_0 is the upstream pressure, ρ the liquid density, Q the flow rate through the device, A_0 and A_t are upstream and throat area respectively. The ratio A_0/A_t is the contraction ratio and values of 16 to 100 have been used. It is clear from the above expression, that for a given liquid with a fixed geometry and p_0, the p_{min} value is determined solely by the magnitude of Q. The higher the magnitude of Q, the lower is the value of p_{min}. The critical value of Q, denoted by Q_c, is given by equating p_{min} with the threshold pressure, p_t, for an

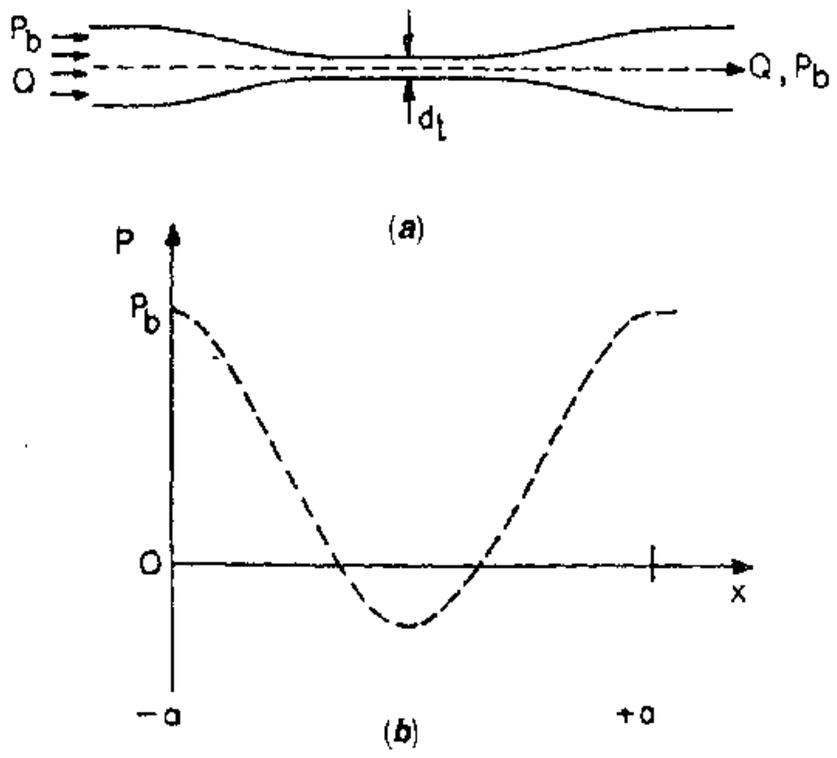

Figure 1. Venturi construction and pressure distribution. *a*, Schematic of venturi. *b*, Ideal pressure distribution.

initial nuclei size of R_0 in equilibrium with the upstream conditions. Assuming isothermal behaviour for the gas inside the bubble, the magnitude of P_t is given by (see for example ref. 2),

$$P_t = P_v - \frac{4\sigma}{3\sqrt{3}\,R_0}\left[1+\frac{(P_0-P_v)R_0}{2\sigma}\right]^{-1/2}. \qquad (2)$$

Here, σ is the coefficient of surface tension and P_v is the vapour pressure at the bulk temperature. Therefore, a nucleus of initial size R_0 will experience vaporous growth at the throat if $P_{min} < P_t$ and it can be computed using the bubble dynamics equation to be introduced later. For this, we assume that the pressure field experienced by a nuclei can be approximated as a half-sine curve indicated in Figure 2. The computed bubble growth and collapse history in response to the pressure field of Figure 2 are shown in Figure 3 for an initial nuclei size of $R_0 = 10\ \mu$m. Depending on the time span, the predicted maximum bubble radii, R_M vary from about 3.3 mm to 6.6 mm. This is a visible size and can

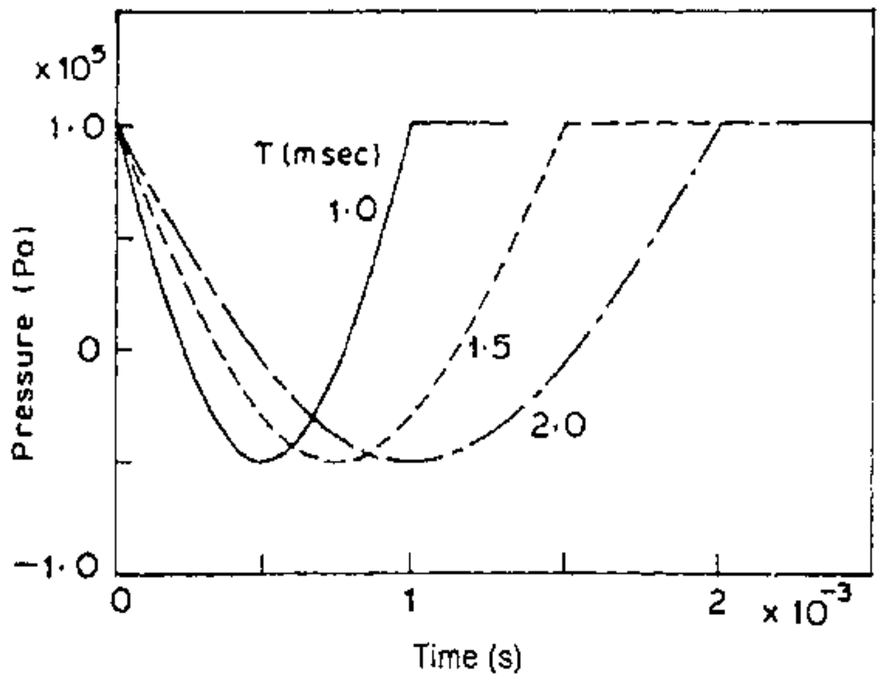

Figure 2. Approximated pressure profiles in the venturi with different time span, $P_{min} = -0.5$ bar. T represents the time span of varying pressure.

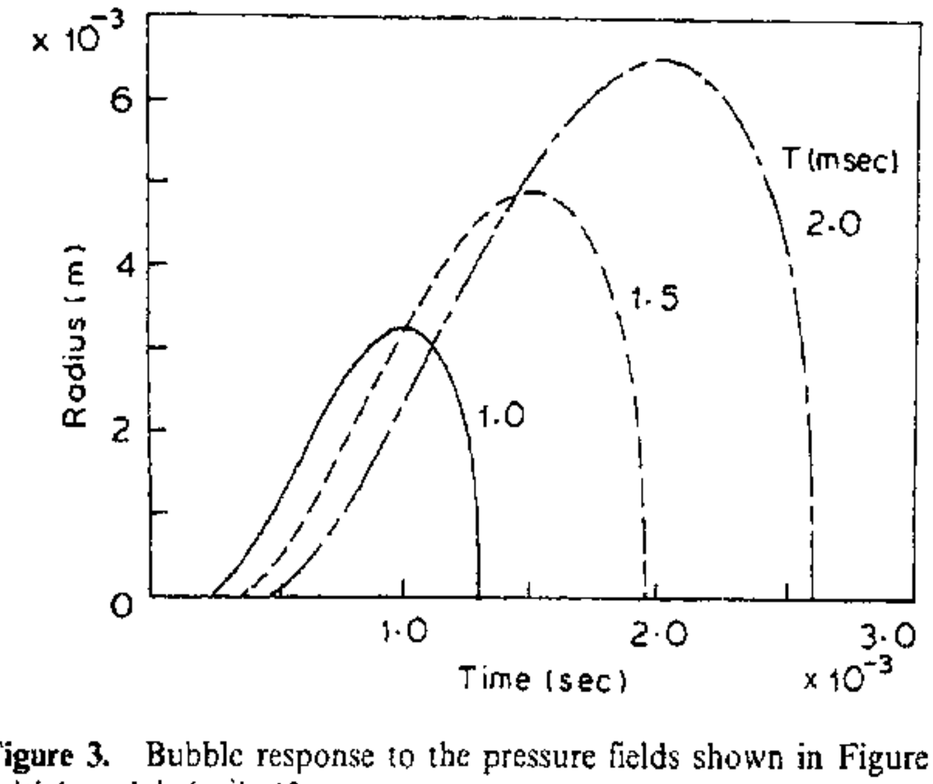

Figure 3. Bubble response to the pressure fields shown in Figure 2. Initial nuclei size is 10 μm.

be termed 'macroscopic' cavitation. It is clear from Figure 3 that the collapse phase is highly nonlinear and bubble wall velocities can even exceed the speed of sound in the liquid medium. It is this violent collapse which is responsible for the observed material damage and intense noise radiation associated with hydrodynamic cavitation. During the collapse phase, the available potential energy at the point of maximum radius is divided into kinetic energy in the liquid, acoustic energy in the form of radiated sound and other losses like heating of the gas inside the bubble if the process is adiabatic. The original solution to the bubble collapse phase was obtained by Lord Rayleigh[3], who equated the potential energy and the kinetic energy mentioned earlier. Therefore, a good measure of the damaging capability of a cavitation bubble is its potential energy at the point of maximum radius; denoting this by PE_M, we can express it in the form,

$$PE_M = \frac{4}{3}\pi R_M^3 P_c. \qquad (3)$$

Here, P_c is the constant collapse pressure and R_M is the maximum radius reached by the bubble during its growth phase. From the above expression it is clear that the maximum bubble radius, R_M is a significant parameter of interest. Second important point from the results presented in Figure 3 is that the total life time of a bubble is approximately equal to the time span of the half-sine curve. In short, two significant features of hydrodynamic cavitation are: maximum bubble sizes of the order of few millimeters and time scales of bubble life time being of the order of few milliseconds. Even though the present conclusions are based on illustrative computations, the orders of magnitude are correct as evident from more extensive computations presented in Paul[4].

Proposed techniques for use of ultrasonics

In the proposed techniques for control or elimination of

hydrodynamic cavitation, we introduce the concepts of two devices, namely, (i) ultrasonic nuclei manipulator (UNM) and (ii) ultrasonic pressure modulator (UPM). The function of UNM is to pre-use existing potential nuclei for hydrodynamic cavitation through their manipulation with ultrasonic waves. This concept is schematically illustrated in Figure 4. Barger[5] demonstrated, that certain types of nuclei can be destroyed or eliminated through repeated cavitation. When a nucleus goes through UNM, it is subjected to an oscillatory pressure field of high frequency. If the amplitude is sufficiently high, it will grow to a maximum size and then collapse violently. Such cavities are termed 'transient cavities' by Flynn[1]; during the collapse phase of such cavities there is every possibility of their fragmenting to smaller size due to instability. The high frequency will ensure that the maximum size reached will not be large and it may be termed 'microscopic' cavitation in contrast to macroscopic cavitation indicated earlier. Once nuclei fragment, they have potential to go into dissolution through a mechanism indicated by Epstein and Plesset[6]. Therefore, the basic function of UNM is to manipulate the existing nuclei to smaller sizes such that their threshold pressures are increased.

It has been indicated earlier that, in a venturi, the throat section is the potential zone of hydrodynamic cavitation. It is conceivable to modulate the pressure field at the throat with the help of an UPM. Thus, an ultrasonic pressure field is superimposed over the basic pressure field and thus nuclei will experience a modulated pressure field. Again, if the frequencies are sufficiently high, it is possible to control the maximum extent of bubble growth such that microcavitation is observed rather than the macrocavitation in the basic pressure field.

Scope of the present work

The basic element of an UNM or UPM will be an ultrasonic projector. The primary scope of the present work is to identify the working parameters of the projector like its frequency of operation and the pressure amplitude. For this we will make extensive use of the solutions to the bubble dynamics equation.

Solutions to the bubble dynamics equation

As indicated earlier, by control of hydrodynamic cavitation we mean here replacing it with relatively less harmful microcavitation. One way to ensure this is to limit the maximum size to which a nucleus brought into the low pressure regions will grow. Therefore, from solutions to the bubble dynamics equation one primary aim is to predict the maximum size to which a bubble will grow under the given pressure field. It turns out that this information can be obtained accurately with less stringent formulation of the bubble dynamics equation than if one was interested in information like maximum temperature or pressure of contents inside the bubble during the last stages of collapse[7]. In the present formulation, the bubble will be assumed to retain its spherical shape throughout its life history and also motions induced in the fluid will be assumed to be incompressible.

Bubble dynamics equation and solution technique

With the assumptions indicated, the derivation of the bubble dynamics equation is contained in several standard textbooks on the subject[8,9]. The resulting equation, known as Rayleigh–Plesset (RP) equation, is

$$R\ddot{R}+\frac{3}{2}\dot{R}^2=\frac{1}{\rho_L}\left[p_{g_0}\left[\frac{R_0}{R}\right]^{3b}+p_v-\frac{2\sigma}{R}-p_\infty(t)\right]. \tag{4}$$

Here, R is the instantaneous bubble radius, ρ_L the liquid density, p_v the vapour pressure, σ the coefficient

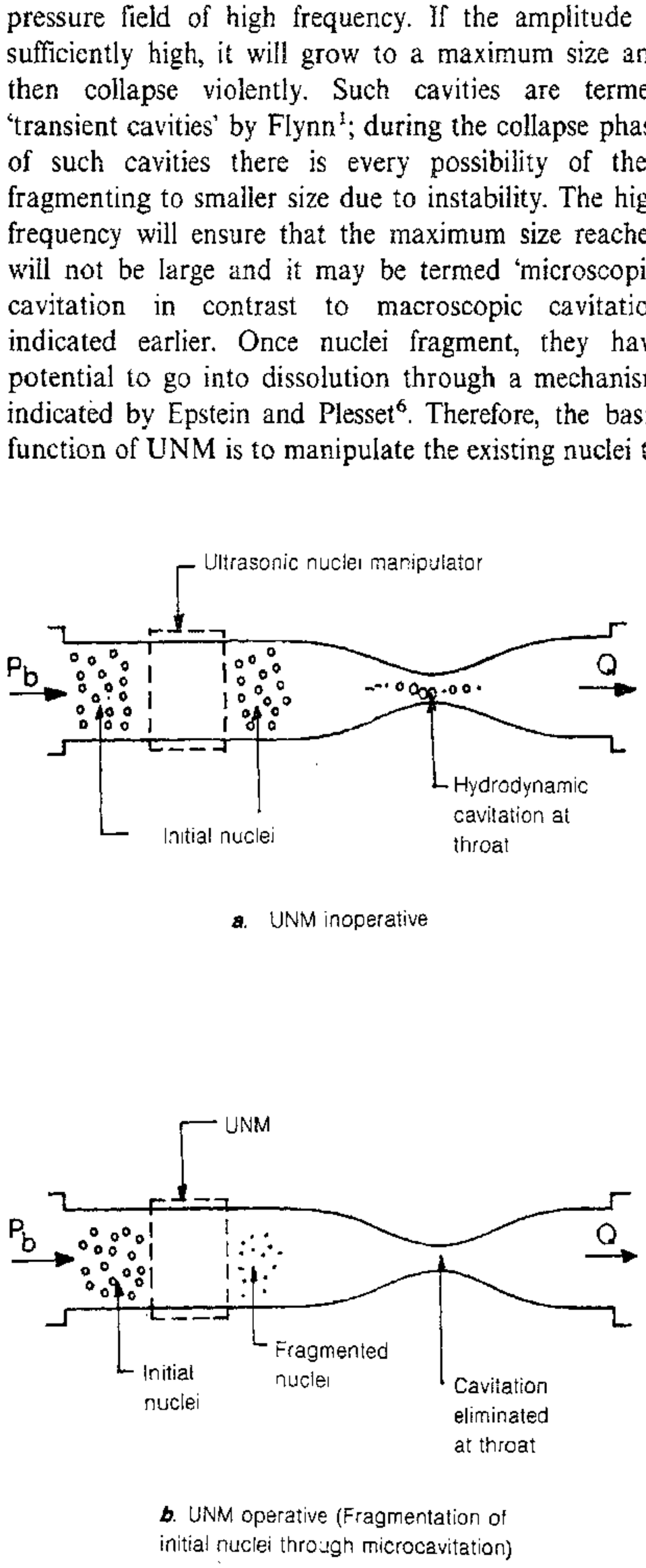

Figure 4. Schematic diagram of proposed experimental set-up with ultrasonic nuclei manipulator and the expected results.

of surface tension, p_{g_0} is the initial gas pressure inside the bubble, R_0 the initial bubble radius, b is a constant equal to 1 for isothermal behaviour of gas and equal to $\gamma = 1.4$ for adiabatic behaviour of the gas taken to be air. In addition, the dots represent the derivative with respect to time and $p_\infty(t)$ is the imposed pressure to which a bubble responds. In the present computations,

$$p_\infty(t) = P_b - P_A \sin \omega t \tag{5}$$

where P_b is the base pressure and P_A and ω are the amplitude and circular frequency of the ultrasonic pressure field with $\omega = 2\pi f$. From initial equilibrium condition we have,

$$p_0 + \frac{2\sigma}{R_0} = p_{g_0} + p_v; \tag{6}$$

this is used to evaluate p_{g_0} for given values of P_0 and R_0. The RP equation was solved as an initial value problem using a subroutine meant for solving stiff differential equations, the details of this including computational flow chart are provided in Paul[4]. The basic bubble dynamics equations being a nonlinear one, it exhibits rich class of solutions. Following Flynn[1,10], we indicate the various types as:

Prompt transient cavities. Here bubbles grow to a maximum size and collapse violently. If this occurs within the first cycle, we term them as 'prompt transient'. The violence is guaged in terms of bubble wall velocity reaching the liquid sonic velocity and the acceleration term being still negative leading the collapse velocity to increase even more. A similar criterion has been used earlier.

Oscillatory transient cavities. Here bubbles oscillate before experiencing a violent collapse and bubble motion is generally a complicated one.

Oscillatory cavities. Here bubbles continue to oscillate within the number of cycles of interest. Typical bubble-radius-versus-time curves for the above types of motions will be presented later.

Bounds for prompt transient cavities

Prompt transient cavities, as defined earlier, collapse violently and hence become potential candidates for fragmentation. Therefore, our interest is to look for bounds in parameters resulting in prompt transient cavities. For this, response of nuclei of initial radii R_0, to an imposed ultrasonic pressure field of amplitude 5 bars and various frequencies was examined. The results are shown in Figures 5 and 6 for isothermal and adiabatic behaviour respectively. The radius-versus-time curves, typical for different kinds of isothermal bubble motion are shown in Figure 7,*a–c* at a

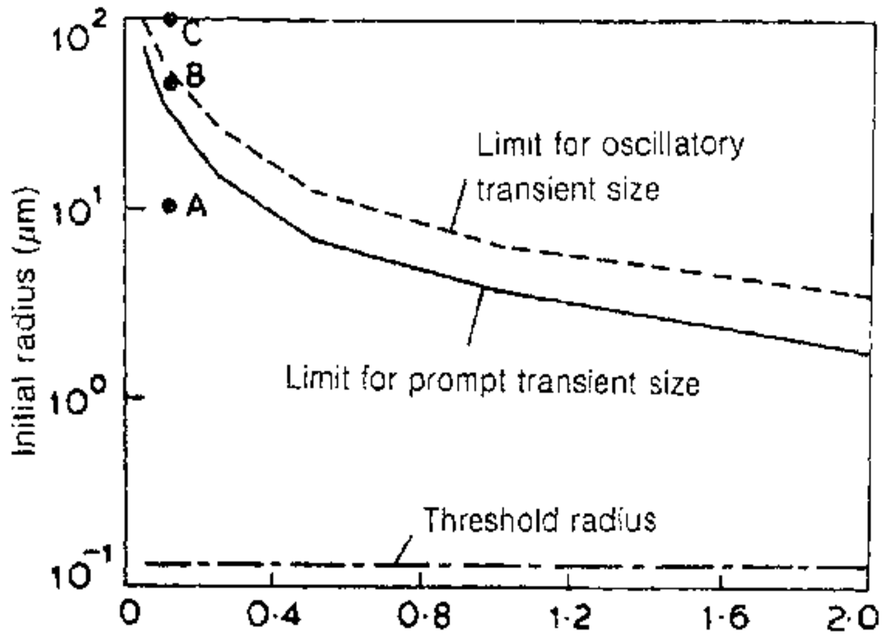

Figure 5. Bounds for prompt and oscillatory transient cavities with isothermal process, frequency dependence of bounds. ($P_A = 5$ bars, P_b and $P_0 = 1$ bar.)

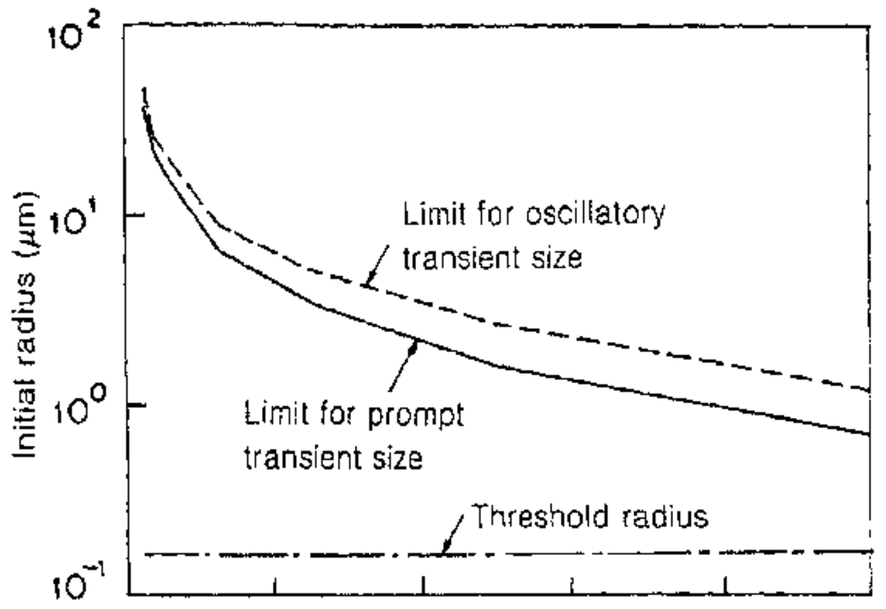

Figure 6. Bounds for prompt and oscillatory transient cavities with adiabatic process, frequency dependence of bounds. ($P_A = 5$ bars, P_b and $P_0 = 1$ bar.)

frequency of 0.1 MHz. The bounds shown in Figures 5 and 6 correspond to 5 cycles. This was chosen in view of the fact that, Flynn[7] has shown that the type of motion exhibited in the first few cycles (like 5) is representive of that which would occur with a continuous wave. Also shown in Figures 5 and 6 are the values of threshold radius for the specified pressure amplitude of 5 bars. This threshold can be defined as the nuclei size for which the critical pressure (given by equation (2) for isothermal behaviour) is just equal to the pressure amplitude imposed. Thus, this is the minimum size of the nuclei that will respond to the imposed pressure field and is frequency independent.

Influence of various parameters on maximum size

Having found the bounds for transient cavitation, we next examine the effect of various other parameters on the maximum size attained by a cavitation nucleus during the growth phase. Figure 8 shows the effect of

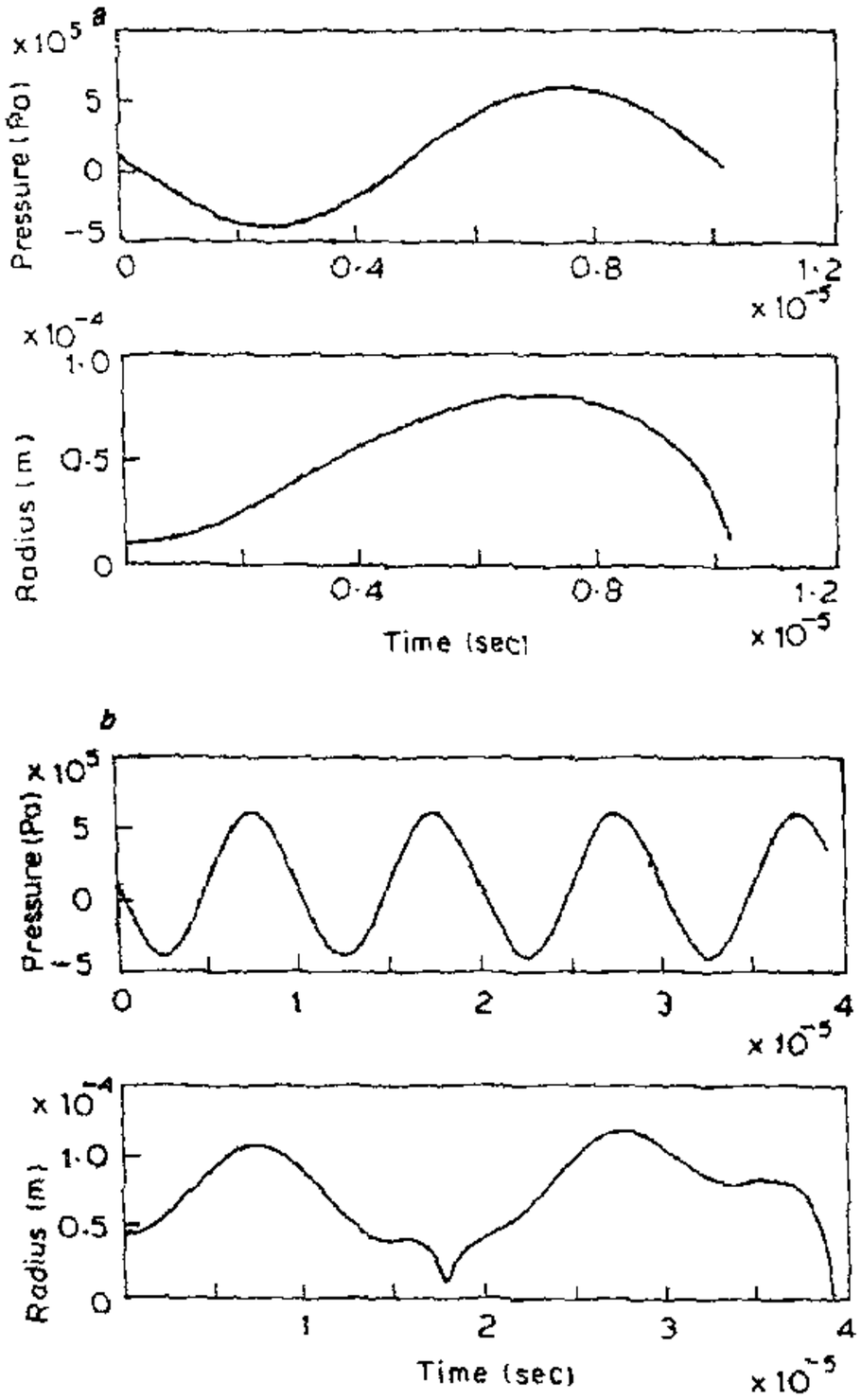

Figure 7. Radius-vs-time curves for different R_0 values, $P_A = 5$ bars, $f = 0.1$ MHz and $P_b = P_0 = 1$ bar. *a*, Corresponding to point A in Figure 5. *b*, Corresponding to point B in Figure 5. *c*, Corresponding to point C in Figure 5. Upper traces show pressure-vs-time curves.

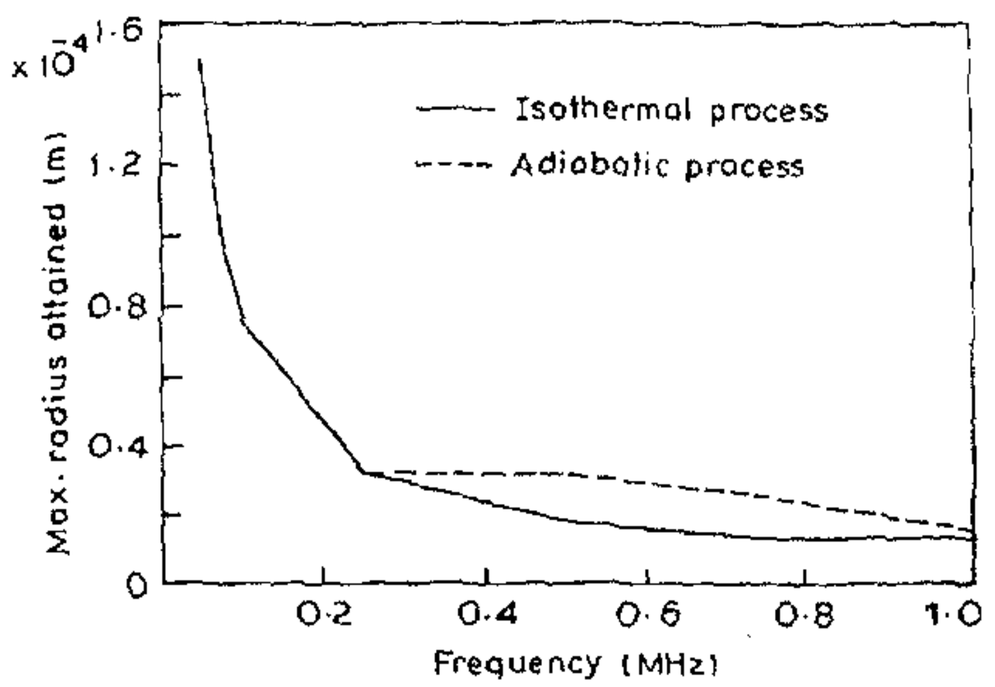

Figure 8. Maximum radius vs frequency, $P_A = 5$ bars, $R_0 = 5$ μm, $P_b = P_0 = 1$ bar. Note for frequencies above 0.35 MHz, the maxima correspond to either oscillatory transient or oscillatory.

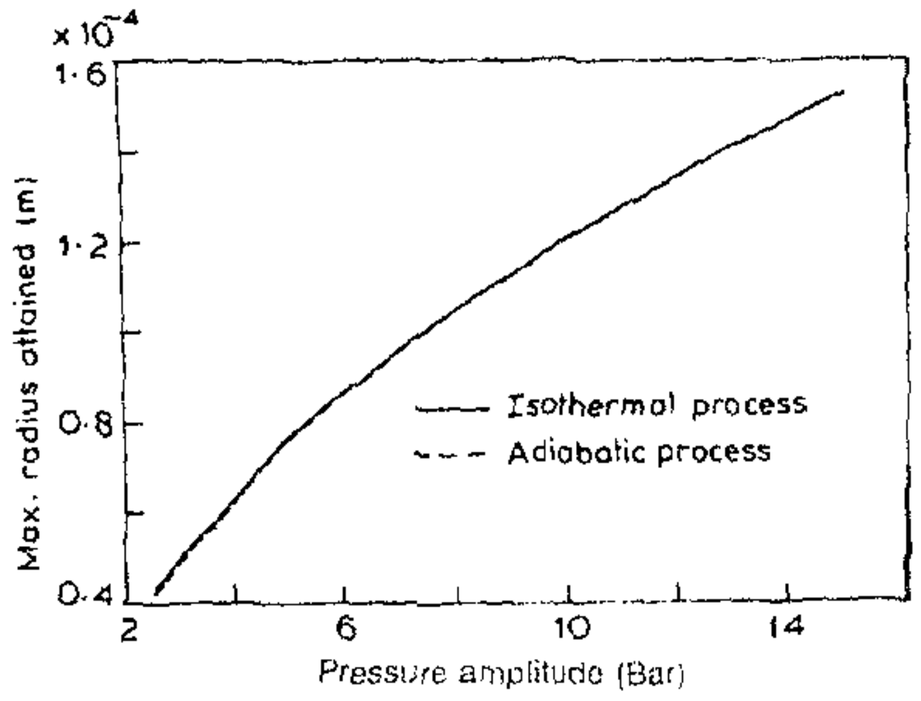

Figure 9. Maximum radius-vs-pressure amplitude. $R_0 = 5$ μm, $P_b = P_0 = 1$ bar, $f = 0.1$ MHz.

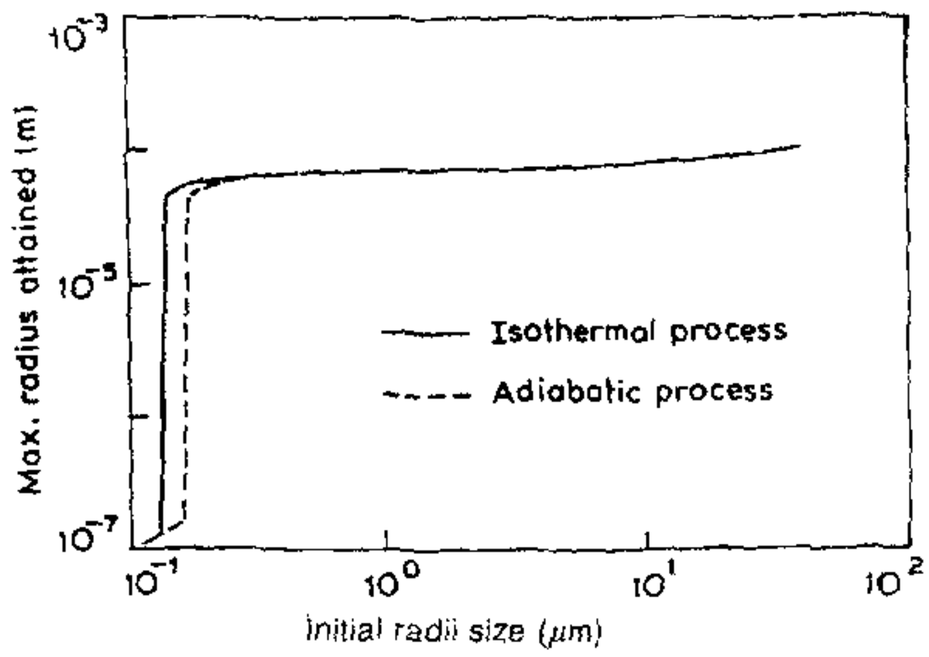

Figure 10. Maximum radius-vs-initial nuclei size. $P_A = 5$ bars, $P_b = P_0 = 1$ bar, $f = 0.1$ MHz.

frequency on the maximum size; the other parameters are fixed as $P_b = 1$ bar (10^5 N/m^2), $P_A = 5$ bars and $R_0 = 5$ μm. The effect of pressure amplitude on R_{max} at a fixed frequency of 0.1 MHz is shown in Figure 9. Finally, the magnitude of R_{max} reached as a function of R_0 with other parameters being fixed as $p_b = 1$ bar, $p_A = 5$ bars and $f = 0.1$ MHz is shown in Figure 10. The results presented consider both the limiting cases of isothermal and adiabatic behaviour for the gas inside the bubble; however, they do not seem to be sensitively dependent on this aspect, since during the growth phase the gas pressure decreases like R^{-3b} and its contribution

to the overall dynamics is thus significantly reduced as growth proceeds.

In the case of venturi, the UNM is to operate upstream of the throat, where the pressure is likely to be near 1 bar and certainly not very low. Hence, P_b has been taken to be 1 bar for results presented in figures 8, 9 and 10; similarly P_0, the pressure at which the nuclei are in equilibrium initially is also taken to be 1 bar. On the other hand, UPM is to operate at the throat of the venturi where pressures may in fact take on negative values. However, nuclei will be still in equilibrium at upstream pressure, P_0. Thus, additional computations were carried out with $P_A = 5$ bars, $f = 0.1$ MHz, $P_0 = 1$ bar, $R_0 = 10\ \mu$m but with $P_b = -1$ bar. The results are shown in Figure 11 and these may be directly compared with those of Figure 7,*a* which are for all parameters being the same except $P_b = +1$ bar. Thus, the comparison noted indicates the effect of base pressure p_b on the maximum size attained.

Discussion of results

It should be noted that the general features of the numerical solutions presented are in excellent quantitative and qualitative agreement with similar earlier studies[7]. However, our emphasis here is quite different and utilizing the numerical results to the bubble dynamics equation obtained presently, an attempt will now be made to suggest operating parameters of the UNM and UPM.

We will first consider the case of UNM. In a practical venturi, cavitation at the throat is likely to occur from a spectrum of nuclei sizes. If ordinary tap-water is used as a working fluid then the size range has a wide spectrum with a peak at about 40 μm (ref. 11). However, a slightly treated sample, like even allowing tap-water to sit quiescently for about half an hour will change the spectrum drastically with mostly smaller size (<10–20 μm) remaining. Therefore, UNM will have to be designed to capture as large a size range as possible to be effective. Again considering our interest being in inducing transient cavitation, we note from Figures 5 and 6 that bound for transient cavitation reduces significantly with increase in frequency. The capture range of initial nuclei, ΔR_c at any frequency can be defined as

$$\Delta R_c = (R_{pt};\ R_t), \tag{7}$$

where R_{pt} is the bound for prompt transient cavities and R_t is the threshold radius. For example, from Figure 6, ΔR_c at 0.1 MHz is approximately (20 μm; 0.17 μm) and it is even higher for the isothermal case (Figure 5). This is sufficiently large from practical considerations; at lower frequencies the capture range will even be higher, but from the results in Figure 8 the maximum size increases sharply. This is to be avoided; in view of this, as a compromise between large capture range and low values for R_{max} a choice of frequency of 0.1 MHz as the operating frequency for UNM seems appropriate.

Next we have to choose the operating pressure amplitude. With reference to this parameter, from the computational results, the following observations can be made:

(i) As shown in Figure 9, the maximum bubble size attained increases with increase in amplitude. This is an unfavourable effect.
(ii) The threshold radius reduces with increase in pressure amplitude. This result can be arrived at by using equation (2). The effect is however marginal above 5 bars but is favourable.
(iii) Higher pressure amplitudes will require higher input power levels to the transducer used for generating ultrasonic pressure field. This effect is unfavourable.
(iv) Limited computations indicated that increase in pressure amplitude effects the bounds for prompt transient cavities in an unfavourable way.

Therefore, the increase of pressure amplitude beyond a certain value is not beneficial. The chosen value of 5 bars, for the computations indicated, seems to be adequate from most considerations. Hence, operating parameters of UNM are fixed as frequency of 0.1 MHz and a pressure amplitude of 5 bars. Such an ultrasonic field can be generated using a piezoelectric transducer. Based on plane wave approximation, the power intensity for 5 bar amplitude is estimated to be 8.33 W cm^{-2}, which is not a large value and not difficult to achieve. The operating scenario of the UNM with the parameters indicated is as follows. Any nuclei with a size in the capture range entering the UNM will go through violent collapse and from the evidence existing, most likely they will fragment to a large

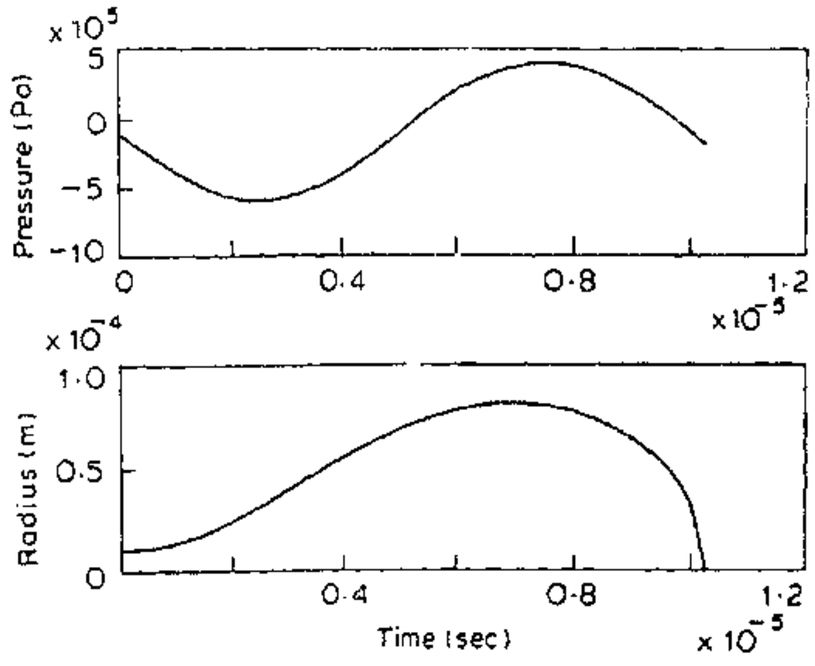

Figure 11. Radius-vs-time curve for $R_0 = 10\ \mu$m, $P_A = 5$ bars $f = 0.1$ MHz, $P_b = -1$ bar and $P_0 = 1$ bar. Upper trace shows pressure-vs-time curve and note the base pressure corresponds to tension.

number of nuclei with smaller sizes. This will occur in the first few cycles; in the subsequent cycles, they could further fragment setting in a cascade effect which will end until the nuclei size becomes close to the threshold radius R_t which is about 0.17 μm for 5 bar pressure amplitude. Thus, in the most efficient fragmentation mode all nuclei in the capture range will end up with a final radii of R_t. Such small nuclei after leaving UNM are likely to be further reduced in size due to dissolution effects associated with surface tension. From the calculations of Epstein and Plesset[6], it is estimated that a bubble of radius 0.17 μm will require about 10^{-4} sec for complete dissolution; in contrast, a bubble of radius 20 μm (being the upper limit of capture range) will require about 100 sec. Therefore, hypothetically it is feasible that all nuclei in a certain size range would be eliminated through microcavitation followed by fragmentation and dissolution. In this case nuclei-free liquid will enter the throat and thus, hydrodynamic cavitation could be avoided at flow rates much higher than the critical flow rate without the UNM operative.

The present state of knowledge about the details of violent phase of bubble collapse does not allow any quantitative estimations or predictions about the fragmentation process. In addition, solutions to the bubble dynamics equation have been obtained with the use of an ideal model for nuclei, namely, an undissolved spherical gas bubble. In reality, other forms of nuclei exist and their response to ultrasonic pressure fields cannot be simply predicted. In view of these weak links, the operation of the UNM will have to be tested experimentally.

We next consider the operating parameters of the UPM. The starting point for this is the comparison of results presented in Figure 7,*a* and Figure 11; in one case the base pressure is +1 bar, whereas in the other it is −1 bar. It is noted that, with $P_A = 5$ bars, the maximum size reached in both cases is about the same. Thus, we can conclude that within limited range, the effect of base pressure on maximum bubble size attained is not significant. In view of this, we can use the extensive results obtained with $P_b = 1$ bar for fixing the operating parameters of UPM. Suppose we assume the same parameters as UNM, then all nuclei in the size range of 0.17 μm to about 20 μm (slightly higher range for isothermal case) will respond and grow to a maximum size not exceeding 0.1 mm (see Figure 10). Even this is an achievement, considering growth up to 6 mm with half-sine curve with a tension of 0.5 bars and time span of 2 msec (see Figure 3). However, what is exciting is the potential operation of UPM at much higher frequencies like 2 MHz. Considering results in Figure 5, at this frequency only nuclei in the range of 0.12 μm to 3.6 μm will respond. Any nuclei with size greater than 3.6 μm simply will go into an oscillatory motion without exhibiting violent collapse. At even higher frequencies, the range will further narrow, however, practical aspects of the transducer design may become significant, since attenuation at these frequencies will be quite high. In the overall sense the power requirements may go up significantly. Therefore, the operating parameters for UPM can be fixed as, f in the range of 1 MHz (with 0.1 MHz being adequate) and P_A of 5 bars.

It was indicated previously, that a good measure of the destructive capability of a cavitation bubble is its potential energy at the point of maximum radius during growth phase. Therefore, it is of interest to compare the magnitude of this measure for microcavitation expected from operation of UNM and UPM and hydrodynamic macrocavitation which otherwise would have occurred. If we denote the respective maximum potential energies as $(PE_M)_U$ and $(PE_M)_H$, then from Figures 10 and 3, we get

$$\frac{(PE_M)_U}{(PE_M)_H} = \left[\frac{0.1 \times 10^{-3}}{5 \times 10^{-3}}\right]^3 \left[\frac{5}{1}\right] = 4 \times 10^{-5}.$$

This follows from predicted maximum radius of 0.1 mm for microcavitation and a collapse pressure of 5 bars; similarly for hydrodynamic cavitation typical maximum radius is taken to be 5 mm and collapse pressure is 1 bar. The ratio noted is indeed small and we can justifiably claim that hydrodynamic cavitation has been controlled through inducement of microcavitation.

Concluding remarks

The success of the use of UNM in controlling hydrodynamic cavitation depends on the hypothesis of efficient fragmentation, about which, currently very little is known. Therefore, actual demonstration would be necessary; what we have achieved, is through, extensive solutions to the bubble dynamics equation come up with suggestion for operating parameters of UNM. Less ambiguities exist about the use of UPM in controlling hydrodynamic cavitation. However, for this the location of low pressure regions must be known accurately. In some class of fluid flows this is feasible, however, in others it may not be. Finally, it should also be mentioned that in the presence of 'copious' supply of nuclei either of the techniques are likely to fail. However, there are several practical situations (like propellers operating at depths in the ocean) where nuclei supply is 'limited' and the techniques described could be effective.

1. Flynn, H. G., *Physics of Acoustic Cavitation in Liquids, Phys. Acoustics* (ed. Mason, W. F.), 1964, **1B**, p. 96.
2. Arakeri, V. H., *Indian J. Technol.*, 1988, **26**, 99.
3. Lord Rayleigh, *Philos. Mag.*, 1917, **34**, 94.

4. Paul, S., *Computational Studies on Single Bubble Cavitation Noise Spectrum*, Rept. No. Me/VHA/HRD-MPA/89-TR-1, Indian Institute of Science. (Also available as M.Sc. thesis.)
5. Barger, J. E., *Thresholds for Acoustic Cavitation*, Tech. Memo. No. 57, Acou. Res. Lab., Harvard University, 1964.
6. Epstein, P. S. and Plesset, M. S., *J. Chem. Phys.*, 1950, **18**, 1505.
7. Flynn, H. G., *J. Acoust. Soc. Am.*, 1982, **72**, 1926.
8. Knapp, R. T., Daily, J. W. and Hammitt, F. G., *Cavitation*, Mc Graw-Hill, 1970.
9. Young, R. F., *Cavitation*, Mc Graw-Hill, 1989.
10. Flynn, H. G. and Church, C. C., *J. Acoust. Soc. Am.*, 1984, **76**, 505.
11. d'Agostino, L., Pham, T. and Green, S., *Comparison of a Cavitation Susceptibility Meter and Holographic Observation for Nuclei Detection in Liquids*, Cavitation and Multiphase Flows Forum (ASME), 1988, p. 20.

21 March 1990

Bamboo, new raw material for phytosterols

Ramesh C. Srivastava
Plant Physiology Section, Department of Life Sciences, Manipur University, Canchipur, Imphal 795 003, India.

Fermented succulent shoots of bamboo (*Bambusa tulda* and *Dendrocalamus giganteus*) are an enriched source of phytosterols. The concentration of phytosterols ranges from 1.6 to 2.8% on dry-weight basis. Fermented bamboo shoots can therefore be used as starting material in the production of steroidal drugs.

OCCURRENCE of various ingredients of nutritional significance in succulent bamboo shoots has been described by many workers[1–5]. Its medicinal importance has also been studied[6–8]. The waste material of sugar industries, press mud, has already been explored as a non-conventional source of sterol to be used for steroidal drugs after its microbial conversion[9–11]. Extensive study on metabolic changes during fermentation of edible bamboo shoots has been made[12, 13], including estimation of a number of metabolites (sugars, organic acids, alcohols, nitrogenous compounds, vitamins, etc.) during fermentation.

The increasing demand for steroidal drugs has resulted in the depletion of various natural resources such as *Dioscoria* and *Solanum*. Hence, an alternative source for a starting material is imperative. In this context phytosterols, which are also used for the production of steroidal drugs, are of some importance. In the present paper, succulent bamboo shoots are proposed as an alternative source of phytosterols.

Bamboo cultivation is practised in many tropical countries. In India, bamboo is grown as a cash crop in the north-eastern part. In Manipur, an area of about 3268 km^2 is covered by bamboo forests[13]. The fermented preparation of bamboo shoot slices, locally called 'soibum', is a highly prized vegetable item (Figure 1). The soibum is manufactured by thin slices of fresh succulent and soft bamboo shoots in specialized containers/chambers for 2–3 months. The fermentation chambers are made up either of bamboo planks or of roasted earthen pots. The inner surface of bamboo chambers are lined with musa leaves and a thin polythene sheet.

The phytosterol was extracted from fresh succulent shoots and also from the fermented product (soibum) obtained from market. The sterol was isolated from oven-dried (60°C) fresh and fermented material. Dry matter was 10–15% of the fresh material. One gram of each sample (fresh and fermented) was crushed with 10 ml alcohol-acetone solution (1 : 1) and centrifuged, the supernatant dried and to the dry residue 10 ml chloroform was added to dissolve phytosterols. The concentration of total phytosterols was determined colorimetrically using the Lieberman–Burchard reaction[14]. Two ml of acetic anhydride-sulphuric acid mixture (30 : 1) was added to 1 ml of phytosterol extract in chloroform; this produces a blue-green colour (λ_{max} 680 nm). Cholesterol was used as standard.

The concentration of total phytosterols was 1.6–2.8% in the dried fermented bamboo shoot samples obtained from different manufacturers. However, its concentration in the dried unfermented (fresh) samples was 0.21–0.39%. The increase in the level of phytosterols in the fermented samples is due to anaerobic digestion by microorganisms that cause degradation of the organic

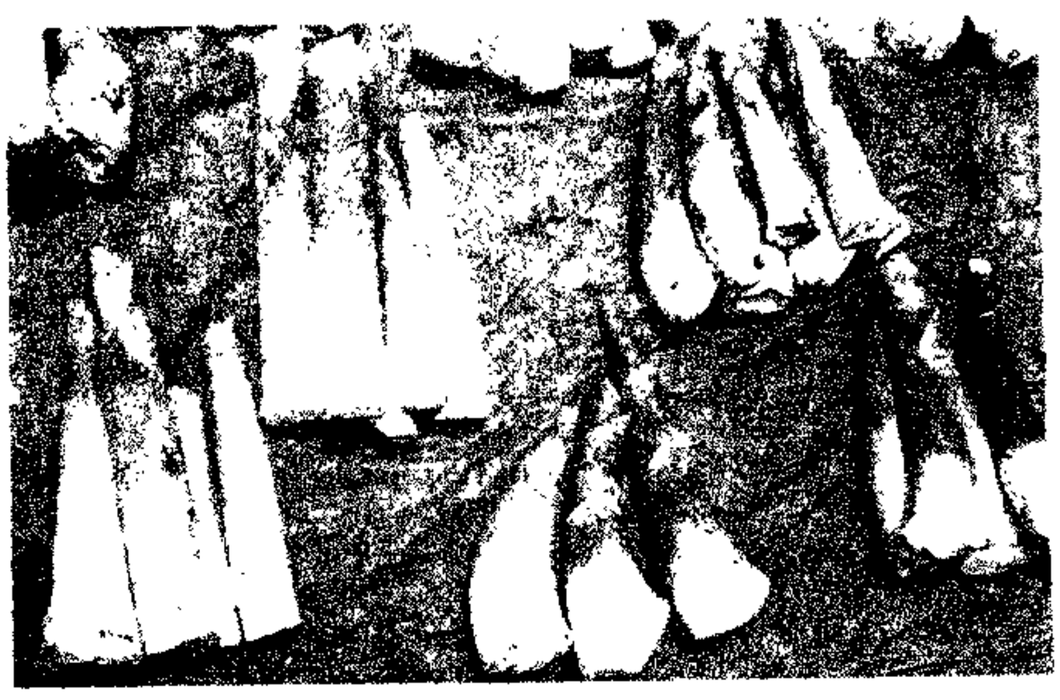

Figure 1. Fresh bamboo shoot (succulent).